ACS OMEGA

Open Access

http://pubs.acs.org/journal/acsodf

Article

Stable Efficient Solid-State Supercapacitors and Dye-Sensitized Solar Cells Using Ionic Liquid-Doped Solid Biopolymer Electrolyte

Subhrajit Konwar,* Sirin Siyahjani Gultekin, Burak Gultekin,* Sushant Kumar, Vinay Deep Punetha, Muhd Zu Azhan Bin Yahya, Markus Diantoro, Famiza Abdul Latif, Ikhwan Syafiq Mohd Noor, and Pramod K. Singh*

Cite This: *ACS Omega* 2024, 9, 39696−39702

Read Online

ACCESS | Metrics & More | Article Recommendations

ABSTRACT: As synthetic and nonbiodegradable compounds are becoming a great challenge for the environment, developing polymer electrolytes using naturally occurring biodegradable polymers has drawn considerable research interest to replace traditional aqueous electrolytes and synthetic polymer-based polymer electrolytes. This study shows the development of a highly conducting ionic liquid (1-hexyl-3-methylimidazolium iodide)-doped corn starch-based polymer electrolyte. A simple solution cast method is used to prepare biopolymer-based polymer electrolytes and characterized using different electrical, structural, and photoelectrochemical studies. Prepared polymer electrolytes are optimized based on ionic conductivity, which shows an ionic conductivity as high as 1.90×10^{-3} S/cm. Fourier transform infrared spectroscopy (FTIR) confirms the complexation and composite nature, while X-ray diffraction (XRD) and polarized optical microscopy (POM) affirm the reduction of crystallinity in biopolymer electrolytes after doping with ionic liquid (IL). Thermal and photoelectrochemical studies further affirm that synthesized material is well stable above 200 °C and shows a wide electrochemical window of 3.91 V. The ionic transference number measurement (t_{ion}) confirms the predominance of ionic charge carriers in the present system. An electric double-layer capacitor (EDLC) and a dye-sensitized solar cell (DSSC) were fabricated by using the highest conducting corn starch polymer electrolyte. The fabricated EDLC and DSSC delivered an average specific capacitance of 130 F/g and an efficiency of 1.73% in one sun condition, respectively.

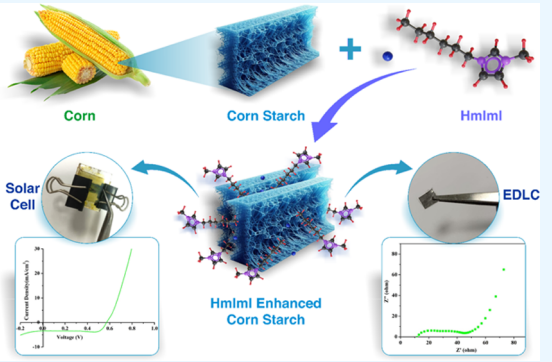

1. INTRODUCTION

Electrolytes are essential in electrochemical energy storage and conversion devices as they are responsible for ion transportation between the electrodes. Traditional electrochemical devices, such as batteries, supercapacitors, and dye-sensitized solar cells, work on aqueous electrolytes. Aqueous electrolytes have high ion transportation and conductivity, increasing the device performance in capacitance, efficiency, and several other parameters. However, some significant limitations related to aqueous electrolytes, such as leakage, evaporation, and bulky design, affect the device stability, design, and self-life.[1−3] The enhancement in capacity of all of the electrochemical devices has played a significant role in research and development along with increased stability and life span. To enhance device performance and overcome the limitations of aqueous electrolytes, replacing aqueous electrolytes with polymer electrolytes is taken into consideration.[4−8]

Polymers are synthetic or naturally occurring macromolecules of a long chain of small molecules known as monomers. Most of the polymers are insulating in nature or show very low ionic conductivities (~10^{-7} to 10^{-8} S·cm^{-1}), which limits their use in electrochemical devices. To enhance the polymers' ionic conductivity, the researchers consider several methods, such as doping nanofillers, salts, or ionic liquids. Ionic liquids are the recent trend in devices like batteries, supercapacitors, and synthesizer-based solar cells. Ionic liquid-doped polymer electrolyte has shown promising results in the performance, stability, and life span of devices.[9−11] Low-viscosity ionic liquid acts as both an ionic species and a plasticizer when doped with a polymer, which enhances the ionic conductivity of the electrolyte and is favorable for the stability and life span of the device. Ionic liquid-doped biopolymer electrolytes have also shown remarkable results in the performance of electrochemical devices.[12−15]

Received: May 22, 2024
Revised: August 29, 2024
Accepted: August 30, 2024
Published: September 12, 2024

Polymers are classified as either biodegradable or nonbiodegradable, with synthetic polymers predominantly falling into the nonbiodegradable category or exhibiting slow degradation. Nonbiodegradable polymer electrolytes pose significant environmental challenges, which constrain their application. Consequently, a growing emphasis is on developing biodegradable and environmentally friendly polymers to meet current ecological and sustainability requirements.[16−18] Starch-based biopolymers, characterized by their biodegradability, renewability, and cost-effectiveness, have garnered considerable interest as alternative materials in research, particularly in comparison with synthetic and nonbiodegradable polymers. These biopolymers are derived from various starch-rich crops, such as rice, wheat, corn, and potatoes, which are cultivated in large quantities. Among these, corn, with its high amylose and amylopectin content, emerges as a promising candidate for replacing existing synthetic polymers due to its advantageous properties.[19−22]

An electric double-layer capacitor (EDLC) is a class of supercapacitors that stores charge using an electric field generated due to the electrostatic separation of dissociated ionic charge to form a Helmholtz double layer. This class of capacitors has the potential to deliver 1000 times more capacitance than conventional dielectric capacitors.[23−26] The higher capacitance is due to the direct ionic charge contribution rather than the dipole contribution of the dielectric polar molecule. Dye-sensitized solar cells (DSSC) are a class of sensitizer-based solar cells. Organic dyes extracted from plants or synthesized artificially in the laboratory are used as a light-absorbing material to produce electrical energy from light energy. These types of solar cells are comparatively cheap and less efficient than silicon solar cells. However, its simple fabrication procedure and cost-effectiveness make it a suitable competitor.[24−26]

In this work, corn starch is used as a host polymer doped with the ionic liquid 1-hexyl-3-methylimidazolium iodide to synthesize polymer electrolytes. These electrolytes are further optimized based on ionic conductivity, and the highest conducting polymer electrolyte film is used to fabricate an EDLC and DSSC. The fabricated EDLC and DSSC have delivered promising results.[27−2829]

2. EXPERIMENTAL SECTION

2.1. Materials Used. Corn starch (CN), potassium iodide (KI), and poly(vinylidene fluoride-*co*-hexafluoropropylene) (PVDF-HFP) are purchased from Sigma-Aldrich; ionic liquid (IL) 1-hexyl-3-methylimidazolium iodide (HmImI) from TCI Chemical India Private Ltd.; flexible graphite sheets from Nickunj Eximp Entp P Ltd., India; fluorine-doped tin oxide (FTO), titania paste, N7 dye, and titanium di-isopropoxide bis (acetylacetonate) from Sigma-Aldrich; double-distilled (DD) water and porous activated carbon are produced in our laboratory.

2.2. Synthesis of Ionic Liquid Biopolymer Electrolyte. The synthesis of ionic liquid biopolymer starts with considering corn starch as a host polymer, salt potassium iodide, and ionic liquid HmImI. Initially, 200 mg of corn starch with 20 mg of glutaraldehyde is fixed and dissolved in DD water to prepare a homogeneous solution. The biopolymer electrolyte is optimized by adding various concentrations of KI into the homogeneous mixture, and the highest ionic conducting composition is achieved at a ratio of 2:1 CN:KI. Moreover, ionic liquid HmImI of different weight concentrations (2, 4, 6, 8, 10, 12, 14, 16, 18, 20) is added to the 2:1 composition of CN:KI to synthesize an ionic liquid biopolymer electrolyte (ILBPE). The solutions are thoroughly stirred for 24 h to achieve a homogeneous mixture and poured into Petri dishes for drying at 50 °C for 12 h. Finally, the films are used for electrical, structural, optical, and thermal analyses, and the highest conducting ILBPE is utilized for application in electrochemical devices.[30,31]

3. DEVICE FABRICATION

3.1. Fabrication of Electric Double-Layer Capacitor. To fabricate EDLC, a flexible thick graphite sheet of 1 cm^2 is cut and used as current collector (CC) electrodes. A slurry of porous carbon (active material) of high specific surface area (600 m^2/g) and PVDF (binder) is prepared in a ratio of 90:10 in 1-methyl-2-pyrrolidinone. The slurry is coated onto the graphite sheets (1 cm × 1 cm) employing a paint brush to form a thin layer of approximately 1 mg/cm^2 and dried at 200 °C for a few hours. The highest conducting ILBPE is sandwiched between two porous carbon electrodes to fabricate the final EDLC.[32−34]

3.2. Fabrication of Dye-Sensitized Solar Cell. To fabricate the DSSC, fluorine-doped tin oxide (FTO) glass was cut into 3 cm^2 pieces, washed thoroughly, and used as current collector electrodes for both the working and counter electrodes of the DSSC. Initially, a thin blocking layer of diluted titanium di-isopropoxide bis (acetylacetonate) is coated upon the FTO glass and dried at 500 °C for 30 min. A thick layer of titania paste is coated over the blocking layer of size 0.25 cm^2 through the doctor's blade method and dried at 500 °C for 30 min. The dried electrode is dipped in a 0.5 mM N7 dye solution for 6−8 h and dried at 50 °C to acquire the working electrode. To another FTO glass diluted solution, 1 mM chloroplatinic acid is coated and dried at 500 °C for 30 min to achieve a platinum-coated counter electrode. The highest conducting ILBPE containing 12 mg of I_2 is sandwiched in between the acquired electrodes to fabricate DSSC.[35,36]

4. RESULTS AND DISCUSSION

4.1. Ionic Conductivity. Electrochemical impedance spectroscopy is carried out for all synthesized films of different compositions of IL. All of the EIS are recorded within a frequency of 10^2−10^6 Hz and an amplitude of 0.05 V at different selected frequencies called decades. The value of current with respect to applied AC voltage is measured along with the phase difference between voltage and current to calculate the actual impedance Z′ and complex impedance Z″. The plot between Z′ and Z″ is the Nyquist plot, and the value of bulk resistance is determined from the graph to evaluate the ionic conductivity of ILBPE with different IL compositions. The ionic conductivity value of all of the ILBPEs is tabulated in Table 1 and plotted in Figure 1.

In the case of electrolytes, conductivity increases with the addition of salt/IL, attaining maxima and decreases. A similar trend is seen for synthesized ILBPE in the literature. The maximum ion conducting value of 1.90 × 10^{-03} S/cm is attained for the composition 2:1:0.24 of CN:KI:IL.

The conductivity of the electrolytes depends mainly on the concentration of ions, mobility, and temperature. Since all of the ILBPE is analyzed at similar temperatures, its effect on mobility and diffusion of extra ions remains unchanged during

https://doi.org/10.1021/acsomega.4c04815
ACS Omega 2024, 9, 39696−39702

Table 1. Variation of the Ionic Conductivity with Different Ionic Liquid Concentrations

HmImI:KICNS	
composition	conductivity S/cm
2	2.53×10^{-04}
4	3.17×10^{-04}
6	5.67×10^{-04}
8	7.14×10^{-04}
10	9.32×10^{-04}
12	1.90×10^{-03}
14	9.17×10^{-04}
16	8.65×10^{-04}
18	6.42×10^{-4}

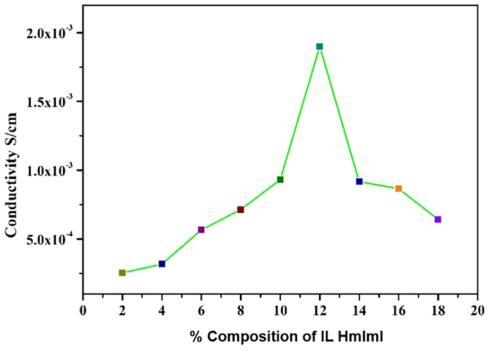

Figure 1. Variation of ionic conductivity for different ionic liquid compositions.

the entire study. The mobility of the ions is primarily affected by the increasing concentration of IL, which leads to interionic interaction because of a higher number of free ions. This higher ion concentration of free ions assisted in ionic conductivity enhancement until 12 wt % of IL, and the decrease in ionic conductivity beyond 12 wt % of IL is due to the steric hindrance among IL ions, which causes difficulty in ionic movement on the way to their respective electrodes.[1,4,9,37] Along with this conductivity enhancement, it also may be due to the H^+ possibility still existing in samples which is more clear from our TGA graph (Figure 7), where it is clearly seen that ∼5 wt % weight loss of water still exists.

Maximum conducting ILBPE is used for the fabrication of EDLC and DSSC. The ionic conductivity concentration is restricted to 18 wt % due to the unavailability of free-standing biopolymer electrolyte film beyond it.

4.2. Ionic Transference Number. Electrolytes, by nature, must be ion-conducting media. The conductivity of electrolytes generally depends on the concentration of cations and anions and the existence of polar molecules. However, a negligible percentage contribution of the electron current could not be avoided. The ionic transference number is the overall contribution of non-Faradaic current due to the ions and polar molecules. In this process, a voltage of 5 kV/m (kilo volt) DC is applied across the polymer ILBPE film for 1 h 20 min until proper polarization. This method is well known as Wagner's DC polarization method and is widely used for the measurement of ionic transference number, which is plotted in Figure 2. From Figure 2, it is observed that the initial current value is comparatively high and the value of the current starts decreasing and stabilizing. The calculated ionic transference

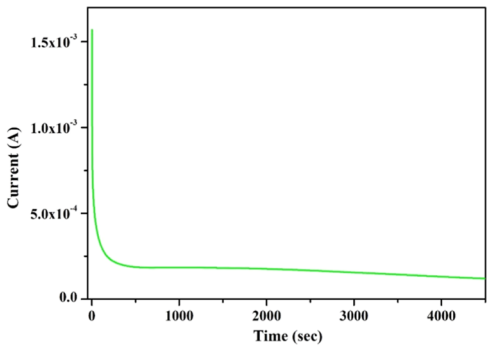

Figure 2. Wagner's polarization plot for maximum conducting ILBPE.

number is as high as 0.96, showing that the ILBPE is predominantly ionic.

4.3. Linear Sweep Voltammetry. A salt/IL in an electrolyte dissociates into a cation and anion and is distributed randomly within the electrolyte. However, all of the cations and anions are not accessible to move because of the formation of paired ions, which restricts their maximum participation in electrode polarization. The paired ion could be separated by means of electric potential and can be termed the threshold potential. In this process, a voltage ranging from −3.5 to 3.5 V is applied across the ILBPE, and the value of current with respect to voltage is recorded and plotted in Figure 3. From Figure 3, it can be seen that the current value is

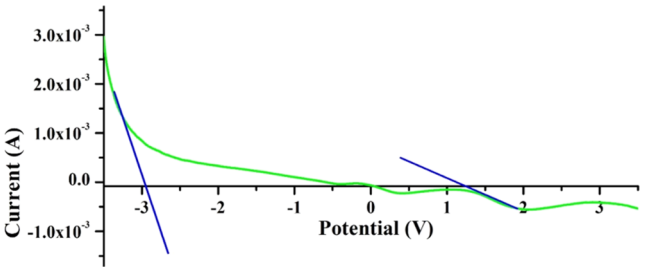

Figure 3. Linear sweep voltammetry plot for maximum conducting ILBPE.

stable with a minimal change in its value within a voltage range of −2.8 to 1.2 V, i.e., 4 V, termed the electrochemical stability window. This is due to the precipitation of the free cation and anion; however, a sudden increase in current over the window is due to the availability of more free ions on account of the applied potential, which leads to the breakdown of the ion pairs. All of the electrical activity performed within the window is reversible; any voltage applied beyond the ESW will act in the breakdown of the ion pair, which regenerates on the removal of the applied potential, contributing to electrical energy loss. Hence, the ESW is a critical parameter for maintaining the performance of electrochemical devices.

4.4. X-ray Diffraction. X-ray diffraction technique is used to study the impact of the addition of salt KI and ionic liquid HmImI in biopolymer corn starch. Figure 4 shows the X-ray diffraction pattern of the pure corn starch, potassium iodide (KI), and the maximum conducting ILBPE. The XRD pattern is recorded over 2θ = 10−80°at a scan rate of 5°/min. The XRD pattern of corn starch shows a broad peak between 11 and 44° with intensity maxima at 20°, showing its semicrystalline nature. The XRD patterns of the potassium iodide show

https://doi.org/10.1021/acsomega.4c04815
ACS Omega 2024, 9, 39696−39702

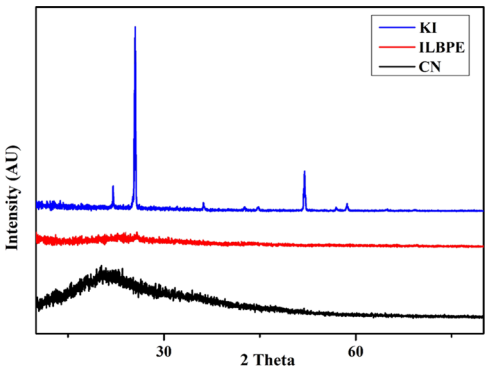

Figure 4. X-ray diffraction pattern of corn starch (CN), potassium Iodide (KI), and maximum conducting ILBPE.

several sharp peaks at various angles, showing its crystalline nature.

In the case of the maximum conducting ILBPE, the broad peak of the CN and the peaks of the salt KI disappeared totally. This is because the biopolymer matrix has changed from a semicrystalline to a completely amorphous nature with the addition of salt KI. The lack of peaks of KI is due to the proper dissociation of salt into cations (K^+) and anions (I^-). The POM analysis also validates the XRD studies, where the same trend is observed.[38,39]

4.5. Fourier Transform Infrared Spectroscopy. Fourier transform infrared (FT-IR) spectroscopy is analyzed to study the interaction of the salt and IL when mixed with the biopolymer corn starch. In this process, FT-IR spectra of CN, KI, IL, and ILBPE are recorded within wavenumbers 4001−652 cm^{-1} and plotted in Figure 5. From Figure 5, a broad peak

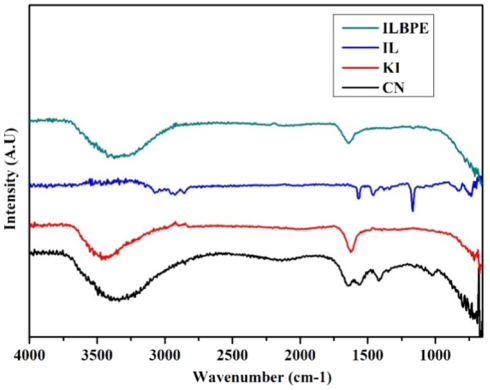

Figure 5. FTIR spectra of corn starch (CN), potassium iodide (KI), ionic liquid (IL), and maximum conducting ILBPE.

expected in the range of 3200−3500 cm^{-1} is observed for all of the host materials, including the ILBPE, indicating the presence of an −OH bond. Similar peaks associated with alkane, alkene, C−H, and O−N bonds are also observed; peaks between 700 and 1700 cm^{-1} are observed in CN and IL as they are organic compounds. The FTIR spectra of ILBPE consist of all of the relevant peaks present in the host material, potassium iodide (KI), and ionic liquid (IL) with diminished intensity and shifting of peaks, which shows the complexation due to the proper dissociation of KI and IL. Close observation and comparative analysis between the host material and ILBPE confirm the composite nature of the ILBPE film.[40,41]

4.6. Polarized Optical Microscopy. Polarized optical microscopy (POM) is a vital imaging technique to identify the crystalline and amorphous regions within the polymer and the polymer electrolyte. Figure 6 shows POM images of CN and

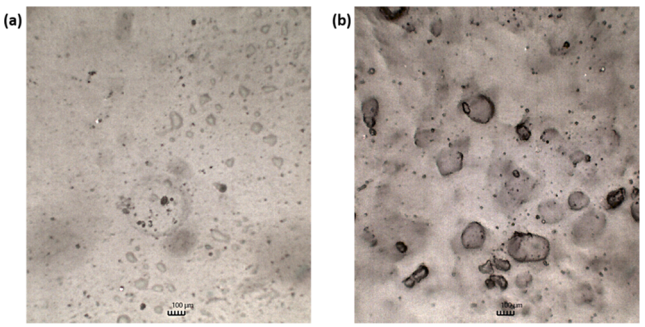

Figure 6. POM images of (a) pure corn starch (CN) and (b) maximum conducting ILBPE.

ILBPE films. From Figure 6a, it is clear that CN contains smaller dark and light patches showing its semicrystalline nature, whereas the large dark patch and small light patch in the ILBPE represent the increase in the amorphous and reduction in the semicrystalline region. The increment in dark patches in Figure 6b confirms the enhancement of the amorphous region with the addition of salt/IL. The same trend is also supported by the conductivity and XRD data.

4.7. Thermogravimetric Analysis. Electrochemical devices are driven by endothermic redox and electrostatic reactions. These devices generate a lot of heat while charging and discharging, which heats the electrolyte to a temperature higher than the surrounding temperature. High-temperature thermal stability hence becomes an important measurement for rapid charging and discharging.

Figure 7 shows the thermogravimetric analysis (TGA) of the ILBPE films. From Figure 7, it is seen that the ILBPE film

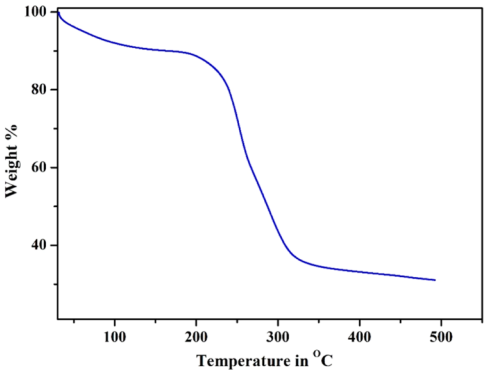

Figure 7. Thermogravimetric analysis for maximum conducting ILBPE.

suffers an initial weight loss of 100, which is due to the presence of a trace of DD water in the films. The ILBPE film is stable to a temperature of 250 °C. The weight loss at higher temperatures is due to decay, precarbonization, and high-temperature reactions. The higher temperature stability of ILBPE makes it suitable for the application of the device at high charging and discharging rates and under extreme temperature conditions.

https://doi.org/10.1021/acsomega.4c04815
ACS Omega 2024, 9, 39696−39702

5. PERFORMANCE OF EDLC

5.1. Low-Frequency Electrochemical Impedance Spectroscopy. Low-frequency electrochemical impedance spectroscopy (LFEIS) analysis of the EDLC cell is carried out within the frequency range of $10^{6}-10^{-2}$ Hz. The Nyquist plot of the EDLC cell is plotted in Figure 8 and is divided into

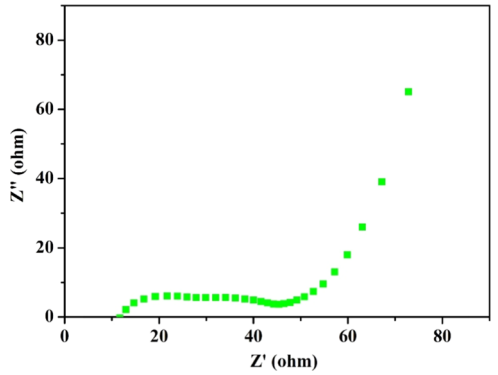

Figure 8. Nyquist plot of the fabricated EDLC in the frequency range of 10^{6} Hz to 10^{-2} Hz.

three different regions. A semicircular region, a linear region making an angle of 40−45°, and finally, a linear region making an angle greater than 45° at three different frequency ranges in between high and low frequencies. The occurrence of a semicircular region is the dielectric nature of the electrolyte, and the two different regions occur due to the electrode−electrolyte interaction and ion absorption at the porous electrode.[37]

The specific capacitance (C_{sp}) of the EDLC cell was calculated to be as high as 135 F/gram at a low frequency of 0.01 Hz. The high specific capacitance is due to the contribution of a highly conducting electrolyte along with the high surface area of porous carbon.

5.2. Cyclic Voltammetry. Cyclic voltammetry (CV)is carried out to study the capacitive nature and the specific capacitance of the EDLC cell. The CV plot plotted in Figure 9

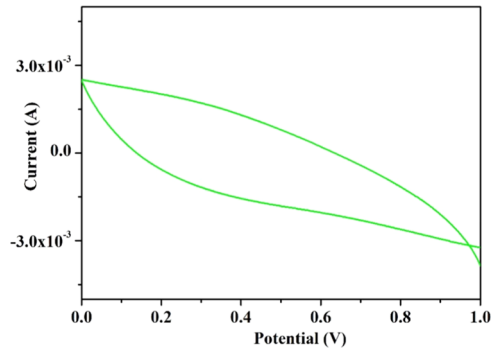

Figure 9. Cyclic voltammetry of fabricated EDLC at 0.01 V/s in the voltage window of 0−1 V.

resembles a rectangular shape, which is observed in the case of EDLC because of the mobility of the ion toward the porous carbon electrode forming the Helmholtz layer in either electrode of the EDLC, causing the nonfaradic process of electrode polarization. CV is carried out at a potential window of 1 V at a scan rate of 0.01 V/s. The fabricated EDLC cell has delivered a specific capacitance of 130 F/gram.

5.3. Constant Current Charging and Discharging. The constant current charging and discharging (CCD) is carried out to evaluate the overall performance of the EDLC cell. In this technique, 4 mA of constant current is applied to charge and discharge the EDLC cell to a potential difference of 1.06 V. The discharge specific capacitance (C_{dsp}), Coulombic efficiency (C_{ef}), specific energy density (E_d), and specific power density (P_d) are calculated from the CCD plot plotted in Figure 10. Figure 10 represents the first 6 CCD cycles, and

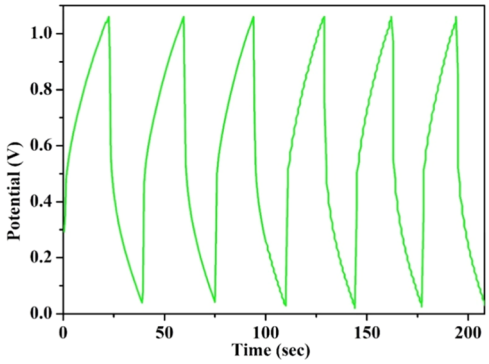

Figure 10. Constant current charging discharging curve for the fabricated EDLC.

the triangular shape resembles that of an EDLC well reported in the literature.[38] It is also observed that voltage increases exponentially from a potential difference of 0.02 to 1.06 V and drops suddenly to 0.62 V and decreases exponentially; the same trend is observed in all six cycles because of the presence of the internal resistance of the EDLC cell. The EDLC cell can deliver a maximum discharge specific capacitance of 110 F/g with a Coulombic efficiency of 79%, followed by an energy density of 37 Wh/kg and a power density of 4080 W/kg.

5.4. Performance of DSSC. The linear sweep voltammetry technique is a widely used method to test the performance of DSSC. In this technique, a sweeping voltage is applied within 0.2−1 V across the DSSCs irradiated at a simulated one sun condition (1000 W/m^2) using a solar simulator by Enlitech at a scan rate of 0.1 V/s by a source meter by Keysight—the third quadrant of the current density (J) vs. voltage (V) graph plotted in Figure 11 is evaluated to measure the overall photon conversion efficiency (η) and the fill factor (FF) of the DSSC. The DSSC has delivered an efficiency of 1.73% and FF. The DSSC cell has produced a short circuit current of 2.52 mA/cm^2 at an open-circuit voltage of 0.68 V, which decreases at a peak load to the current of 2.39 mA/cm^2 and voltage of 0.63 V.

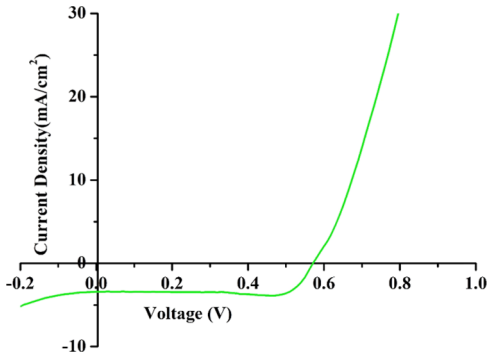

Figure 11. J-V characteristics of the fabricated DSSC.

https://doi.org/10.1021/acsomega.4c04815
ACS Omega 2024, 9, 39696−39702

6. CONCLUSIONS

A mixed ionic system consisting of inorganic salt KI and organic ionic liquid HmImI-doped biopolymer electrolyte is successfully synthesized with a high ionic conductivity as high as 10^{-3} aS/cm. The EIS study confirms that doping ionic liquid (IL) into the biopolymer electrolyte increases conductivity, which reaches a maximum and then decreases. Conductivity enhancement is generally governed by the availability of free ionic charges or depressed crystallinity, while decreases in conductivity are affirmed by ion pairing. FTIR confirms the complexation and composite nature of the films. Ionic transference number measurement clearly confirms a predominantly ionic nature with an ESW as high as 4 V, allowing this system to be widely applied. XRD and POM studies clearly indicate enhancement in amorphousity by suppressing the crystallinity of biopolymer electrolytes. The thermal stability of the biopolymer electrolyte from thermogravimetric analysis over 200 °C claims its high-temperature stability. The fabricated electrochemical devices like sandwiched EDLC with the highest ionic conductivity are tested with tools like EIS, CV, and CCD for deciding the specific capacitance as high as 130 F/g while fabricated DSSC is tested using LSV tools and have delivered an efficiency of 1.73% at one sun condition, respectively.

■ ASSOCIATED CONTENT

Data Availability Statement

All data generated or analyzed during this study are included in this published article.

■ AUTHOR INFORMATION

Corresponding Authors

Subhrajit Konwar − *Center for Solar Cells & Renewable Energy, Department of Physics, Sharda University, Greater Noida 201310, India; Department of Physics, Noida Institute of Engineering and Technology, Greater Noida 201306, India*; Email: subhrajitkonwar@gmail.com

Burak Gultekin − *Solar Energy Institute, Ege University, Bornova, Izmir 35100, Turkey*; orcid.org/0000-0002-8804-7844; Email: burak.gultekin@ege.edu.tr

Pramod K. Singh − *Center for Solar Cells & Renewable Energy, Department of Physics, Sharda University, Greater Noida 201310, India*; orcid.org/0000-0002-3155-6621; Email: pramodkumar.singh@sharda.ac.in

Authors

Sirin Siyahjani Gultekin − *Faculty of Engineering, Department of Chemical Engineering Canakkale, Onsekiz Mart University, Canakkale 17100, Turkey; Solar Energy Institute, Ege University, Bornova, Izmir 35100, Turkey*; orcid.org/0000-0002-6385-8034

Sushant Kumar − *Center for Solar Cells & Renewable Energy, Department of Physics, Sharda University, Greater Noida 201310, India*

Vinay Deep Punetha − *Centre of Excellence for Research, P P Savani University, Kosamba 394125, India*

Muhd Zu Azhan Bin Yahya − *Faculty of Defence Science and Technology, Universiti Pertahanan Nasional Malaysia (UPNM), 57000 Kuala Lumpur, Malaysia*

Markus Diantoro − *Department of Physics, Faculty of Mathematics and Natural Science, Universitas Negeri Malang, Malang 65145, Indonesia*

Famiza Abdul Latif − *Faculty of Applied Sciences, Universiti Teknologi MARA, 40450 Shah Alam, Malaysia*

Ikhwan Syafiq Mohd Noor − *Physics Division, Centre of Foundation Studies for Agricultural Science, Universiti Putra Malaysia (UPM), 43400 Serdang, Selangor Darul Ehsan, Malaysia*; orcid.org/0000-0003-0983-782X

Complete contact information is available at: https://pubs.acs.org/10.1021/acsomega.4c04815

Author Contributions

All authors have contributed equally to this manuscript.

Notes

The authors declare no competing financial interest.

■ ACKNOWLEDGMENTS

The author, Pramod K. Singh (PKS), is thankful to the CSTUP (CST/D-1041) for financial assistance.

■ REFERENCES

(1) Dhawan, R.; Singh, A.; Kumar, S.; Dhapola, P. S.; Alheety, M. A.; Yahya, M. Z. A.; Serguei, S. Futuristic Approach Towards Replacement of Aqueous Electrolyte with Solid Polymer Electrolyte for Supercapacitor Applications. *J. Electron. Mater.* **2023**, *52* (7), 4295−4301.

(2) Sangwan, B.; Kumar, S.; Singh, A.; Pandey, S. P.; Singh, P. K.; Singh, R. C.; Tomar, R. Modified Poly(Vinyl Alcohol) Based Polymer Electrolyte for Dye Sensitized Solar Cells (DSSCs). *Macromol. Symp.* **2023**, *407* (1), No. 2100462.

(3) Kumar, S.; Singh, P. K.; Agarwal, D.; Singh Dhapola, P.; Sharma, T.; Savilov, S. V.; Arkhipova, E. A.; Singh, M. K.; Singh, A. Structure, Dielectric, and Electrochemical Studies on Poly(Vinylidene Fluoride-Co-Hexafluoropropylene)/IonicLiquid 1-Ethyl-3-Methylimidazolium Tricyanomethanide-Based Polymer Electrolytes. *Phys. Status Solidi A* **2022**, *219* (7), No. 2100711.

(4) Mathela, S.; Kumar, S.; Singh, P. K.; Chandra Singh, R.; Shukla, P.; Singh, V.; Noor, I.; Kakroo, S.; Madkhli, A. Y.; Tomar, R. Ionic Liquid Dispersed Highly Conducting Polymer Electrolyte for Supercapacitor Application: Current Scenario and Prospects "ICSEM 2021.". *High Perform. Polym.* **2022**, *34* (6), 652−672.

(5) Sharma, T.; Gultekin, B.; Dhapola, P. S.; Sahoo, N. G.; Kumar, S.; Agarwal, D.; Jun, H. K.; Singh, D.; Nath, G.; Singh, P. K.; Singh, A. Ionic Liquid Doped Poly (Methyl Methacrylate) for Energy Applications. *J. Mol. Liq.* **2022**, *352*, No. 118494.

(6) Qiu, Y.; Zhang, X.; Tian, Y.; Zhou, Z. Machine Learning Promotes the Development of All-Solid-State Batteries. *Chin. J. Struct. Chem.* **2023**, *42* (9), No. 100118.

(7) Xue, W.; Deng, W.; Chen, H.; Liu, R.; Taylor, J. M.; Li, Y.; Wang, L.; Deng, Y.; Li, W.; Wen, Y.; et al. MOF-directed Synthesis of Crystalline Ionic Liquids with Enhanced Proton Conduction. *Angew. Chem., Int. Ed.* **2021**, *60* (3), 1290−1297.

(8) Song, H.; Xue, S.; Chen, S.; Wang, Z.; Song, Y.; Li, J.; Song, Z.; Yang, L.; Pan, F. Polymeric Wetting Matrix for a Stable Interface between Solidstate Electrolytes and Li Metal Anode. *Chin. J. Struct. Chem.* **2022**, *41* (5), 2205048−2205054.

(9) Sharma, H.; Tomar, R.; Konwar, S.; Singh, P. K.; Chandra Singh, R.; Kumar, S.; Singh, A.; Agarwal, D.; Yahya, M. Highly Efficient Ionic-liquid Based Solid Polymer Electrolyte for Energy Device (RAFM 2022). *High Perform. Polym.* **2023**, *35* (1), 56−62.

(10) Singh, A.; Sharma, T.; Dhapola, P. S.; Kumar, S.; Singh, D.; Nath, G.; Singh, V.; Alheety, M. A.; Kakroo, S.; Singh, P. K. Ionic Liquid Doped Solid Polymer Electrolyte: Synthesis, Characterization and Applications ICSEM-2021. *High Perform. Polym.* **2022**, *34* (6), 645−651.

(11) Singh, D.; Kumar, S.; Singh, A.; Sharma, T.; Dhapola, P. S.; Konwar, S.; Arkhipova, E. A.; Savilov, S. V.; Singh, P. K. Ionic

https://doi.org/10.1021/acsomega.4c04815
ACS Omega 2024, 9, 39696−39702

Liquid−Biopolymer Electrolyte for Electrochemical Devices. *Ionics* **2022**, *28* (2), 759−766.
(12) Tabasum, S.; Younas, M.; Zaeem, M. A.; Majeed, I.; Majeed, M.; Noreen, A.; Iqbal, M. N.; Zia, K. M. A Review on Blending of Corn Starch with Natural and Synthetic Polymers, and Inorganic Nanoparticles with Mathematical Modeling. *Int. J. Biol. Macromol.* **2019**, *122*, 969−996.
(13) Rayung, M.; Aung, Min. M.; Ahmad, A.; Su'ait, Mohd. S.; Abdullah, L. C.; Ain Md Jamil, Siti. N. Characteristics of Ionically Conducting Jatropha Oil-Based Polyurethane Acrylate Gel Electrolyte Doped with Potassium Iodide. *Mater. Chem. Phys.* **2019**, *222*, 110−117.
(14) Shi, J.; Shi, B. Environment-Friendly Design of Lithium Batteries Starting from Biopolymer-Based Electrolyte. *NANO* **2021**, *16* (05), No. 2130006.
(15) Jothi, M. A.; Vanitha, D.; Bahadur, S. A.; Nallamuthu, N. Promising Biodegradable Polymer Blend Electrolytes Based on Cornstarch:PVP for Electrochemical Cell Applications. *Bull. Mater. Sci.* **2021**, *44* (1), 65.
(16) Muchakayala, R.; Song, S.; Wang, J.; Fan, Y.; Bengeppagari, M.; Chen, J.; Tan, M. Development and Supercapacitor Application of Ionic Liquid-Incorporated Gel Polymer Electrolyte Films. *J. Ind. Eng. Chem.* **2018**, *59*, 79−89.
(17) Konwar, S.; Singh, A.; Singh, P. K.; Singh, R. C.; Rawat, S.; Dhapola, P. S.; Agarwal, D.; Yahya, M. Highly Conducting Corn Starch Doped Ionic Liquid Solid Polymer Electrolyte for Energy Storage Devices. *High Perform. Polym.* **2023**, *35* (1), 63−70.
(18) Mei, B.-A.; Munteshari, O.; Lau, J.; Dunn, B.; Pilon, L. Physical Interpretations of Nyquist Plots for EDLC Electrodes and Devices. *J. Phys. Chem. C* **2018**, *122* (1), 194−206.
(19) Salau, A. O.; Olufemi, A. S.; Oluleye, G.; Owoeye, V. A.; Ismail, I. Modeling and Performance Analysis of Dye-Sensitized Solar Cell Based on ZnO Compact Layer and TiO2 Photoanode. *Mater. Today: Proc.* **2022**, *51*, 502−507.
(20) Surana, K.; Bhattacharya, B. Dye Sensitized and Quantum Dot Sensitized Solar Cell. In *Recent Advances in Thin Film Photovoltaics*; Springer, 2022; pp 131−149.
(21) Mehmood, U.; Aslam, H. Z.; Al-Sulaiman, F. A.; Al-Ahmed, A.; Ahmed, S.; Malik, M. I.; Younas, M. Electrochemical Impedance Spectroscopy and Photovoltaic Analyses of Dye-Sensitized Solar Cells Based on Carbon/TiO_2 Composite Counter Electrode. *J. Electrochem. Soc.* **2016**, *163* (5), H339−H342.
(22) Chen, K.; Wang, L.; Tong, H.; Tao, L.; Wang, K.; Zhang, Y.; Zhou, X. Mesoporous TiO2 Hollow Microsphere Constructed with TiO2 Nanospheres: High Light Scattering Ability and Enhanced Photovoltaic Performance for Dye-Sensitized Solar Cells. *J. Mater. Sci.: Mater. Electron.* **2020**, *31* (20), 17659−17669.
(23) Singh, R.; Singh, P. K.; Singh, V.; Bhattacharya, B. Quantitative Analysis of Ion Transport Mechanism in Biopolymer Electrolyte. *Opt. Laser Technol.* **2019**, *113*, 303−309.
(24) Jothi, M. A.; Vanitha, D.; Sundaramahalingam, K.; Nallamuthu, N. Utilisation of Corn Starch in Production of "Eco Friendly" Polymer Electrolytes for Proton Battery Applications. *Int. J. Hydrogen Energy* **2022**, *47* (67), 28763−28772.
(25) Wang, J.; Liang, Y.; Zhang, Z.; Ye, C.; Chen, Y.; Wei, P.; Wang, Y.; Xia, Y. Thermoplastic Starch Plasticized by Polymeric Ionic Liquid. *Eur. Polym. J.* **2021**, *148*, No. 110367.
(26) Ahuja, H.; Dhapola, P. S.; Rahul; Sahoo, N. G.; Singh, V.; Singh, P. K. Ionic Liquid (1-Hexyl-3-Methylimidazolium Iodide)-Incorporated Biopolymer Electrolyte for Efficient Supercapacitor. *High Perform. Polym.* **2020**, *32* (2), 220−225.
(27) Devi, L. S.; Das, A. B. Effect of Ionic Liquid on Sol-Gel Phase Transition, Kinetics and Rheological Properties of High Amylose Starch. *Int. J. Biol. Macromol.* **2020**, *162*, 685−692.
(28) Yadav, N.; Hashmi, S. A. High Energy Density Solid-State Supercapacitors Based on Porous Carbon Electrodes Derived from Pre-Treated Bio-Waste Precursor Sugarcane Bagasse. *J. Energy Storage* **2022**, *55*, No. 105421.
(29) Rosli, N. A. H.; Loh, K. S.; Wong, W. Y.; Yunus, R. M.; Lee, T. K.; Ahmad, A.; Chong, S. T. Review of Chitosan-Based Polymers as Proton Exchange Membranes and Roles of Chitosan-Supported Ionic Liquids. *Int. J. Mol. Sci.* **2020**, *21* (2), 632.
(30) Ren, F.; Wang, J.; Xie, F.; Zan, K.; Wang, S.; Wang, S. Applications of Ionic Liquids in Starch Chemistry: A Review. *Green Chem.* **2020**, *22* (7), 2162−2183.
(31) Salama, A.; Hesemann, P. Recent Trends in Elaboration, Processing, and Derivatization of Cellulosic Materials Using Ionic Liquids. *ACS Sustainable Chem. Eng.* **2020**, *8*, 17893−17907.
(32) Chen, P.; Xie, F.; Tang, F.; McNally, T. Ionic Liquid (1-Ethyl-3-Methylimidazolium Acetate) Plasticization of Chitosan-Based Bionanocomposites. *ACS Omega* **2020**, *5* (30), 19070−19081.
(33) Alday, P. P.; Barros, S. C.; Alves, R.; Esperança, J. M.; Navarro-Segarra, M.; Sabaté, N.; Silva, M. M.; Esquivel, J. P. Biopolymer Electrolyte Membranes (BioPEMs) for Sustainable Primary Redox Batteries. *Adv. Sustainable Syst.* **2020**, *4* (2), No. 1900110.
(34) Nath, G.; Singh, P. K.; Dhapola, P. S.; Sharma, T.; Patil, G. P.; Jadhav, C. D.; Singh, A.; Konwar, S.; Savilov, S. V.; Singh, D.; Yahya, M. Z. A. Biodegradable Methylcellulose Biopolymer-Derived Activated Porous Carbon for Dual Energy Application. *Mater. Renewable Sustainable Energy* **2022**, *11* (3), 241−250.
(35) Mallik, A. K.; Shahruzzaman, M.; Zaman, A.; Biswas, S.; Ahmed, T.; Sakib, M. N.; Haque, P.; Rahman, M. M. Fabrication of Polysaccharide-Based Materials Using Ionic Liquids and Scope for Biomedical Use. In *Functional Polysaccharides for Biomedical Applications*; Elsevier, 2019; pp 131−171.
(36) Sun, Z.; Yang, L.; Zhang, D.; Song, W. High Performance, Flexible and Renewable Nano-Biocomposite Artificial Muscle Based on Mesoporous Cellulose/Ionic Liquid Electrolyte Membrane. *Sens. Actuators, B* **2019**, *283*, 579−589.
(37) Kumar, S.; Singh, M. K.; Yahya, M. Z. A.; Noor, I. S. M.; Singh, P. K. Structural, Electrochemical, and Dielectric Studies of Phytagel and 1-Ethyl-3-Methylimidazolium Tricyanomethanide-Based Bio-Polymer Electrolytes. *Zast. Mater.* **2024**, DOI: 10.62638/ZasMat1050.
(38) Lakshmi, N.; Chandra, S. Ion Transport in Some Solid State Proton Conducting Composites Studied from Volta Cell Emf and Complex Impedance Spectroscopy. *Bull. Mater. Sci.* **2002**, *25*, 197−201.
(39) Hoang, H. M.; Pham, T. B. V.; Grampp, G.; Kattnig, D. R. Exciplexes versus Loose Ion Pairs: How Does the Driving Force Impact the Initial Product Ratio of Photoinduced Charge Separation Reactions? *J. Phys. Chem. Lett.* **2014**, *5* (18), 3188−3194.
(40) Kumar, S.; Singh, D.; Singh, A.; Srivastava, M.; Kumar, S.; Singh, R.; Yadav, T.; Alheety, M. A.; Singh, P. K. Waste Peanut Shells Derived Activated Carbon for Dual Electrochemical Applications. *Energy Storage* **2024**, *6*, No. e571.
(41) Kumar, S.; Singh, P. K.; Punetha, V. D.; Singh, A.; Strzałkowski, K.; Singh, D.; Yahya, M. Z. A.; Savilov, S. V.; Dhapola, P. S.; Singh, M. K. In-Situ N/O-Heteroatom Enriched Micro-/Mesoporous Activated Carbon Derived from Natural Waste Honeycomb and Paper Wasp Hive and Its Application in Quasi-Solid-State Supercapacitor. *J. Energy Storage* **2023**, *72*, No. 108722.

https://doi.org/10.1021/acsomega.4c04815
ACS Omega 2024, 9, 39696−39702